ACS Energy LETTERS

http://pubs.acs.org/journal/aelccp

Effects of Atmospheric Gases on Li Metal Cyclability and Solid-Electrolyte Interphase Formation

Evelyna Wang, Sunita Dey, Tao Liu, Svetlana Menkin, and Clare P. Grey*

Cite This: *ACS Energy Lett.* 2020, 5, 1088−1094

Read Online

ACCESS | Metrics & More | Article Recommendations | Supporting Information

ABSTRACT: For Li−air batteries, dissolved gas can cross over from the air electrode to the Li metal anode and affect the solid-electrolyte interphase (SEI) formation, a phenomenon that has not been fully characterized. In this work, the impact of atmospheric gases on the SEI properties is studied using electrochemical methods and ex situ characterization techniques, including X-ray photoelectron spectroscopy, X-ray diffraction, Fourier transform infrared spectroscopy, and scanning electron microscopy. The presence of O_2 significantly improved the lithium cyclability; less lithium is consumed to form the SEI or is lost because of electrical disconnects. However, the SEI resistivity and plating overpotentials increased. Lithium cycled in an "air-like" mixed O_2/N_2 environment also demonstrated improved cycling efficiency, suggesting that dissolved O_2 participates in electrolyte reduction, forming a homogeneous SEI, even at low concentrations. The impact of gas environments on Li metal plating and SEI formation represents an additional parameter in designing future Li-metal batteries.

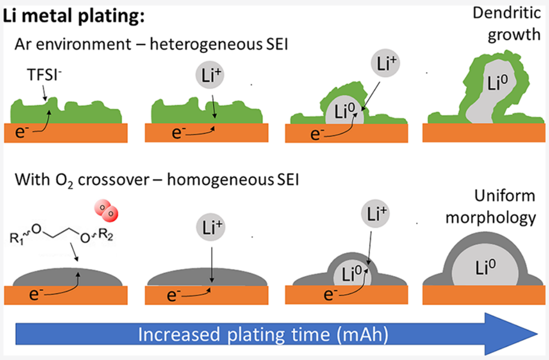

As demand for high-performance energy storage devices continues to grow, "beyond lithium-ion" battery technologies, such as conversion-type chemistries and lithium metal anodes, are necessary to meet these needs.[1] Li−air batteries, for instance, promise extremely high energy capacities, with estimated theoretical values up to 3500 Wh/kg and practical capacities in the range of 500−1000 Wh/kg.[2−6] Since the first report of a Li−air battery, various electrodes, catalysts, electrolytes, and additives such as redox mediators and H_2O have been employed to lower charge overpotentials, suppress side reactions, and improve the cyclability.[7−14] Although significant progress has been made at the positive electrode, the generally irreversible reactions that occur at the Li metal anode have not been fully characterized.[2,15]

The reduction potential of lithium is very low, such that it will spontaneously decompose electrolyte, resulting in the growth of a solid-electrolyte interphase (SEI).[16] An ideal SEI is electronically insulating to prevent continuous electrolyte decomposition, yet ionically conductive to lithium ions.[16,17] In a Li−air battery, SEI formation is affected by dissolved gas diffusing from the positive electrode to the Li anode, analogous to undesirable polysulfide shuttling in Li−S batteries and gas crossover in fuel cells (schematic 1);[18−23] the saturated O_2 concentration and O_2 diffusion constant for 1 M LiTFSI in tetraglyme were estimated to be around ~0.6 mM and 10^{-7}cm^2/s in 1 atm dry air at 25 °C, respectively.[24−26] Furthermore, while the solubilities of other atmospheric gases are less studied, they also affect SEI formation because of the reactivity of Li metal.[27−30] Several studies have shown that atmospheric gases, including N_2, can affect lithium cycling.[31−33]

The stability of the lithium SEI is crucial to battery performance and lithium cyclability.[16,34−36] Discrepancies in previous literature on the positive or negative impact of gas crossover on SEI formation and lithium stability have yet to be explained.[19,20,31,32,37−39] Many reports state the necessity of using a protected Li metal anode or SEI-forming additives to enable cycling in the presence of O_2.[9,20,40−44] Furthermore, the effect of O_2 partial pressures has not been explored, yet this is relevant to Li metal batteries prepared in dry room environments. These gaps in understanding necessitate a systematic investigation of SEI and lithium plating in various atmospheric gas environments.

Received: February 4, 2020
Accepted: March 10, 2020
Published: March 10, 2020

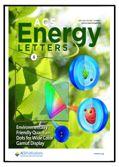

https://dx.doi.org/10.1021/acsenergylett.0c00257
ACS Energy Lett. 2020, 5, 1088−1094

Scheme 1. Schematic of the Li Metal Electrode during Charge in a Li–Air Battery Where Gas Crossover from the Positive Electrode Can Participate in SEI Formation

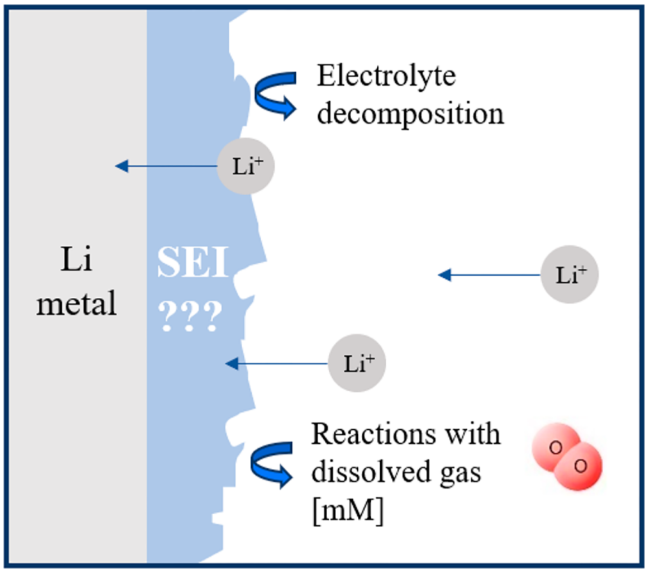

In this study, lithium metal was plated/stripped onto a copper substrate while exposed to O_2, Ar, and N_2 environments. Ex situ techniques were used to characterize the SEI, including scanning electron microscopy (SEM), Fourier-transform infrared spectroscopy (FT-IR), X-ray diffraction (XRD), and X-ray photoelectron spectroscopy (XPS). The presence of O_2 gas during Li plating, while increasing the interfacial resistance, resulted in uniform nucleation and dendrite suppression and enabled good Coulombic efficiencies. A homogeneous SEI consisting of large LiOH domains is likely formed as opposed to a heterogeneous layer formed of many microphases. In mixed O_2/N_2 environments, Li plating morphologies and cyclability were also improved, but without a notable increase in resistance. These findings indicate that gas crossover in Li–air batteries and other Li metal batteries plays a significant role in SEI homogeneity and overall performance.

Electrochemical Cycling of Li Cu Cells. Lithium metal was plated/stripped in various atmospheric gases with the Swagelok design shown in Figure S1. An initial 2.5 mAh/cm^2 of lithium was plated onto the Cu substrate, then subjected to 20 stripping–plating cycles at 10% of the initial capacity, all under galvanostatic conditions (Figure 1a). At the end, all available lithium was stripped from the Cu. Coulombic efficiencies (abbreviated as CE) were calculated using the Aurbach method, which provides an average efficiency over the whole experiment (Figure S2).[38] Overpotential was averaged from the voltage plateaus during plating. The electrolyte was 1 M LiTFSI in tetraglyme.

The Li plating and stripping tests performed in O_2, Ar, and N_2 atmospheres showed stark differences in overpotential and capacity loss. Samples in Ar, while initially cycling with a low overpotential, showed a large jump in polarization after the first 9 cycles (Figure 1a), indicating that no more lithium can be removed from the Cu electrode.[34,35] Almost 40% irreversible loss in capacity occurred in a single plating/stripping cycle (Figure 1d). This poor performance is in agreement with previous studies using ether electrolytes.[45]

By contrast, O_2 crossover greatly improved the CE (Figure 1b); however, there was a large increase in overpotential (Figure 1c). Interestingly, O_2 improved the performance in carbonate-based electrolytes without increasing the overpotential (Figure S3). This suggests that improved plating/stripping efficiencies with O_2 are not solely due to high overpotentials, the high overpotentials increasing Li nucleation density according to classical nucleation and growth theory.[17] An N_2 gas environment slightly improved the CE as well, without a drastic increase in plating overpotential (Figure 1b).

Impedance spectroscopy was performed following 20 plating–stripping cycles, and the data were fit with an equivalent circuit model (Figure S4). Larger impedances were observed for the SEI formed in O_2, consistent with the trend in overpotentials. The shape of the impedance was also different in the O_2 sample, indicating differences in SEI structure and ion transport mechanism.

Ex Situ Morphology and Composition Studies After Cycling. SEM images were taken to investigate the effect of gas crossover on the cycled morphology (Figure 2a). After the cycling and stripping of all the available lithium, electrically isolated Li dendrites were visible in the Ar sample, which explains the large capacity losses (Figure 1b). This dead Li was observed in the XRD spectra for Ar and N_2 samples (Figure

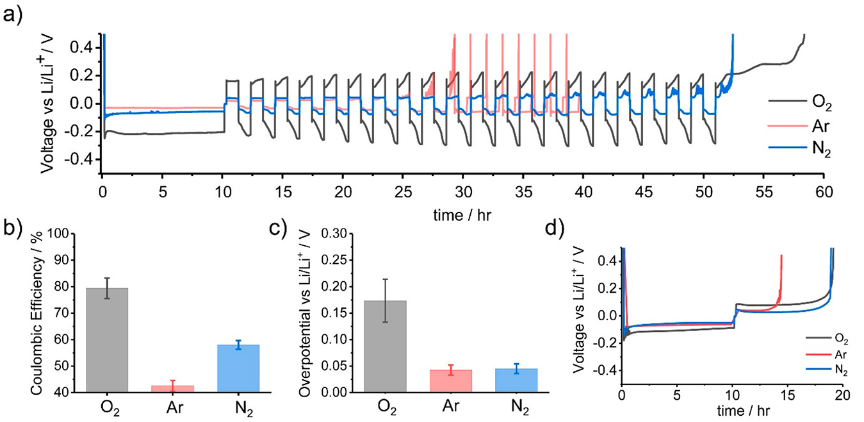

Figure 1. Electrochemical cycling of Li|Cu cells. (a) Potential versus time plot for galvanostatic cycling tests performed in O_2, Ar, and N_2. (b) Coulombic efficiency and (c) plating overpotentials. Four cells were repeated in each gas environment, and error bars show standard deviations. (d) Galvanostatic plating–stripping for one cycle. Current densities of 0.25mA/cm^2 were used.

https://dx.doi.org/10.1021/acsenergylett.0c00257
ACS Energy Lett. 2020, 5, 1088–1094

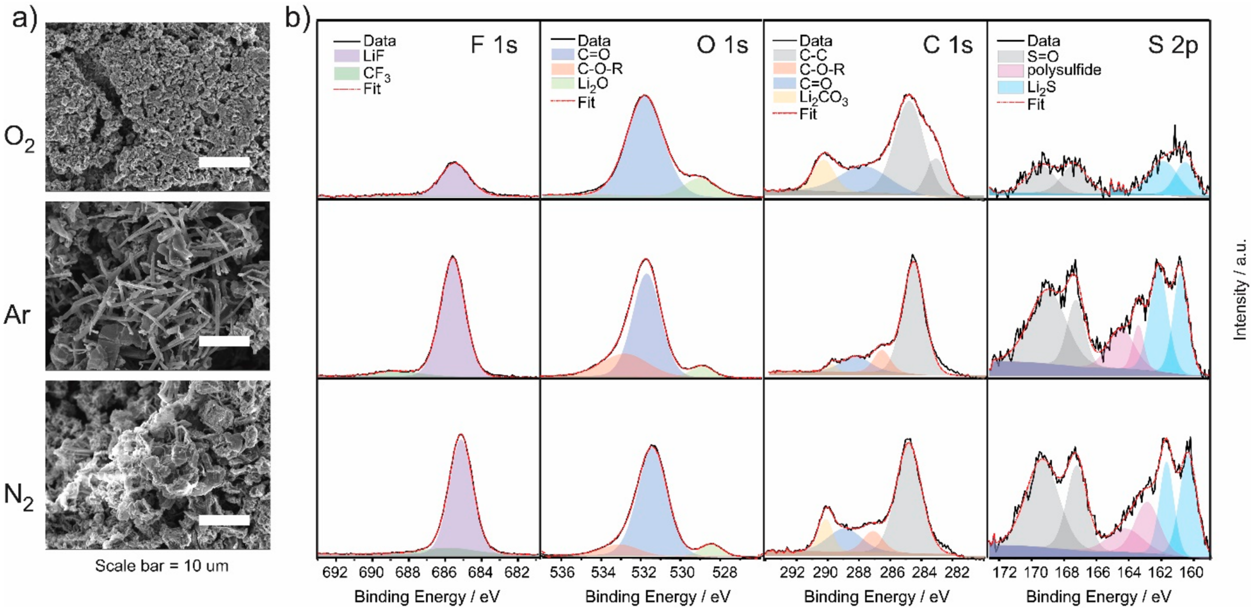

Figure 2. SEI morphology and composition studies. (a) SEM images and (b) XPS spectra for the SEI formed in various gas environments after cycling.

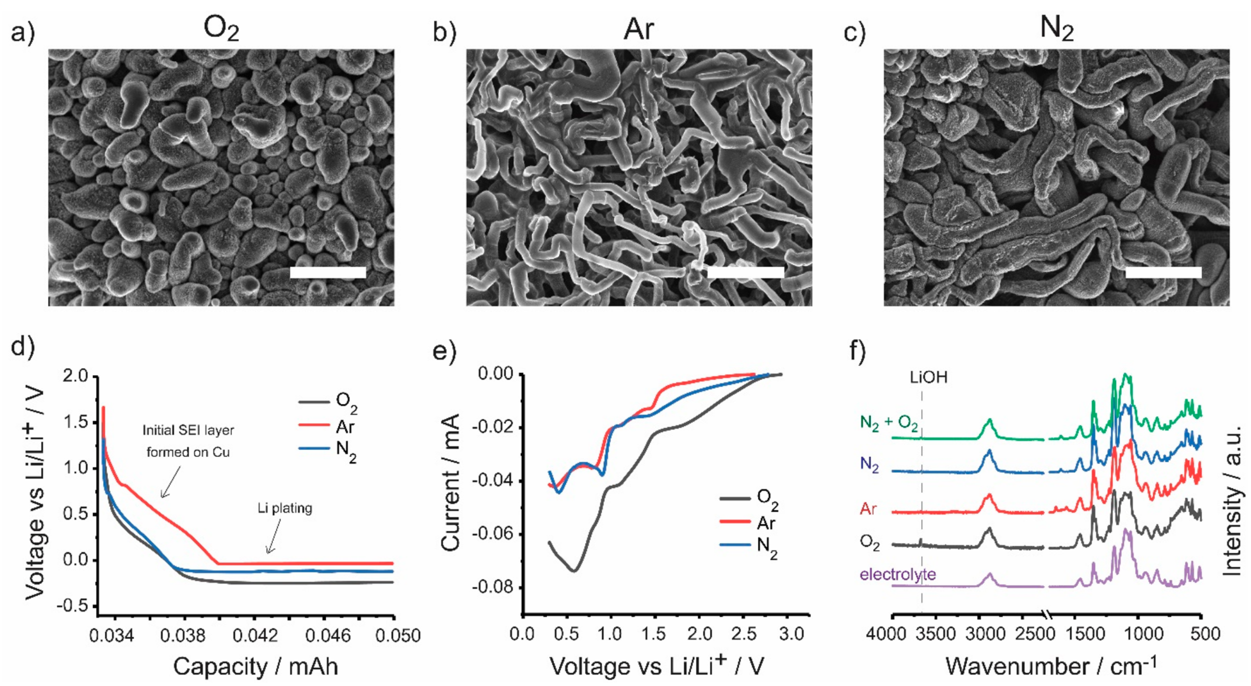

Figure 3. Effect of O_2 on Li nucleation. (a−c) SEM images of the first Li plating. Scale bar = 10 μm. (d) Voltage versus capacity during galvanostatic plating. (e) Linear sweep voltammetry to 0.3 V vs Li/Li$^+$ and (f) subsequent FTIR measurements of the Cu electrode.

S5). In an O_2 environment, the cycled morphology was more uniform and less porous (Figures 2a and S6), which correlates with the weaker Li signal seen by XRD (Figure S5) and the higher CE observed (Figure 1b).

Ex situ XPS was used to characterize the SEI components: for all samples, salt decomposition products, including LiF, Li_2O, and Li_2S, were identified (Figure 2b).[36,46] Peak positions are well aligned with previous studies.[47,48] These peaks increased with depth profiling while the C−C peaks decreased (Figure S7 and Table S4), consistent with widely accepted SEI models: more inorganic components closer to the SEI/Li metal interface.[16] From the F 1s and S 2p spectra, relative peak intensities of LiF (purple) and Li_2S (cyan) were much larger for the SEIs formed in Ar and N_2 than in O_2 (Figure 2b and Tables S5−S9), and total atomic concentrations showed more F, N, and S content as well (Figures S7 and S8). Online electrochemical mass spectrometry results also indicate increased fluoride species in Ar and N_2 samples compared to O_2 (Figure S9).

There were fewer salt reduction products in the SEI formed with O_2, and LiOH was observed from the XRD and FTIR spectra (Figures S3 and S10). These peaks were absent in the Ar and N_2 samples. In addition, Li_2CO_3 (Figure 2b, yellow) was detected with larger relative intensities in the O_2 sample; a

C 1s peak at 283 eV, attributed to Li−C species, was also detected in the O_2 sample.[48,49] Although LiF-rich SEIs reportedly improve Li metal anode stability, the poor Coulombic efficiencies in Ar samples, despite high LiF content, suggest that other species—likely LiOH—and mechanisms such as SEI uniformity may play a large role in controlling lithium plating and stripping.[50−53]

Studies of the Initial Li Deposition. The initial Li plating of 2.5 mAh/cm^2, prior to cycling, resulted in round, particulate Li morphologies for O_2 samples (Figure 3a). In an Ar environment, whisker-like dendrites were formed (Figure 3b). Both uniform nuclei and thick dendrites were observed for N_2 samples (Figure 3c). We hypothesize that O_2 affects the Cu surface, which subsequently affects lithium nucleation.[17,54] In galvanostatic plating, the low reduction potentials of lithium dictate that electrolyte is first reduced; this continues until an electrically insulating layer is formed across the Cu surface, preventing further electrolyte reduction.[16,36] In the presence of O_2, less charge was irreversibly consumed to form this initial surface layer (Figures 3d and S11); a similar effect is seen with SEI-forming additives such as fluorethylene carbonates.[51,54] The peak beginning around 2.5 V in the voltammetry sweep corresponds to O_2 reduction on the Cu electrode prior to Li nucleation (Figure 3e).

In order to identify surface species formed prior to Li nucleation, FTIR was measured on Cu electrodes biased to 0.3 V vs Li/Li$^+$ under O_2, Ar, and N_2 (Figure 3f). LiOH was observed only in O_2 samples. No significant amount of LiOH was observed when biasing to 0.3 V in an N_2 environment and subsequently exposing to O_2 at open-circuit potential (Figure 3e, green). This indicates that LiOH was formed electrochemically. These LiOH morphologies are visible in SEM images of the Cu surface when plating in O_2 environments (Figure S12a), whereas under Ar, the Cu surface remains rougher (Figure S12b).

To test the hypothesis that the LiOH-rich SEI formed in O_2 promotes more uniform Li nucleation, we explored a pretreatment method whereby the cell was first cycled in O_2 for 5 cycles before purging and continuing to cycle in Ar. Cells cycled in Ar have low initial CE of 60% which drops rapidly to below 5% after 5 cycles (Figure S13), whereas similar cells cycled in O_2 maintained a CE of >90% for more than 60 cycles (where cycling was stopped). Cycling in O_2 and then swapping to an Ar atmosphere extended the cycle life to 30 cycles while maintaining high efficiencies of >90% (Figure S13). However, the cell still fails, indicating that O_2 continues to play a role in SEI formation during cycling.

Effect of Mixed Gas on SEI Formation. Lithium was next cycled in mixed O_2/N_2 environments to determine the effect of O_2 at different O_2 partial pressures. Impressively, CE values in O_2/N_2 environments were comparable to those of samples cycled in O_2 (Figure 4a), dropping to 80% for a 25:75 O_2/N_2 ratio. The initial Li nuclei in a mixed O_2/N_2 environment were also round and nondendritic (Figures 4c and S14a for the 25:75 and 50:50 ratio, respectively). The plating overpotentials drop steadily with decreasing O_2/N_2 ratio (Figure 4b), and the overall SEI composition for the 25:75 sample is closer to that cycled in N_2 (Figure 4d). LiOH is still detected by FTIR and SEM (Figure S14).

Discussion. The XPS, XRD, and FTIR results all suggest that the SEI formed in Ar and N_2 contains multiple inorganic products from LiTFSI reduction. This heterogeneous SEI, following the mosaic model,[16] leads to nonuniform ion diffusion through the SEI, uneven Li plating, and dendritic growth,[45,50] consistent with the observed dendritic morphologies (Figure 3b). In constrast, the O_2 SEI contains large LiOH crystallites that form before the onset of plating; this SEI results in much smoother and rounder Li deposits, also coated with LiOH. The positive effects of O_2 persist even when either swapping to an Ar atmosphere after the initial cycling (for up to 25 cycles) or when using a lower O_2 partial pressure.

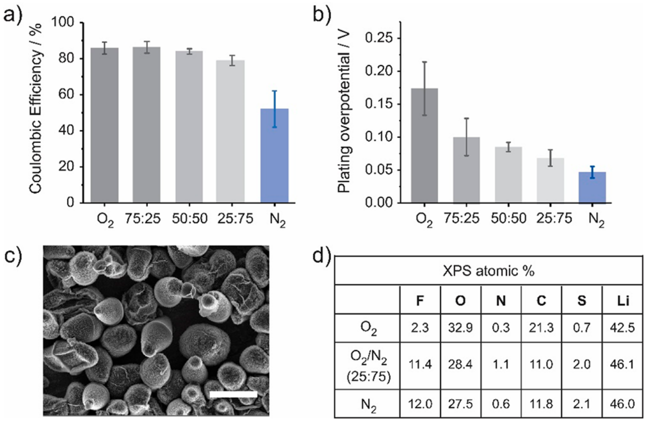

XPS atomic %						
	F	O	N	C	S	Li
O_2	2.3	32.9	0.3	21.3	0.7	42.5
O_2/N_2 (25:75)	11.4	28.4	1.1	11.0	2.0	46.1
N_2	12.0	27.5	0.6	11.8	2.1	46.0

Figure 4. Effect of mixed gas on SEI formation. (a) Coulombic efficiencies and (b) plating overpotentials as a function of O_2/N_2 ratio. (c) SEM image after Li plating in O_2/N_2 (25:75). Scale bar = 10 μm. (d) XPS atomic percentage for the SEI formed in O_2, N_2, and 25:75 O_2/N_2.

From the impedance measurements and equivalent circuit modeling,[55] bulk SEI resistances were similar across all samples; however, the SEI formed in O_2 had a larger resistance modeled via a second resistor/capacitor component, likely relating to grain boundaries and the formation of the LiOH layer. Lower grain boundary resistivities were observed in Ar and N_2 samples by more than 60 Ω, indicating higher total ionic conductivity and is reflected in the lower plating overpotentials (Figure 1c). The higher grain boundary resistivity observed in the O_2 sample is consistent with a homogeneous and full covering layer of LiOH (SEM, Figure S12) that ions must travel through as discussed in more detail in the Supporting Information (Figure S4 and Table S1).

Two mechanisms have been proposed for SEI formation in the presence of O_2 (Figure S15). The first involves the reduction of O_2 to form superoxides and then Li_2O_2, which can then attack the ether solvent, forming Li-carbonates, Li alkoxy species, and LiOH.[38,56] Li_2O_2 may directly deposit on the Cu surface as well; however, this was not detected with the characterization methods used. Although glymes have improved stability against reduced oxygen species compared to carbonate solvents, the highly reductive potentials during lithium plating may also affect the reactivity of glymes, resulting in radical formation, the radicals then react with O_2.[21,57−59] The increased Li_2CO_3 content for SEI formed in O_2 is consistent with increased glyme decomposition (Figure 2b). Oxygen and nitrogen can also chemically react with lithium metal; this appears to be a minor effect compared to electrochemical SEI formation as shown in EDX measurments of Li metal exposed to gas environments under OCV conditions (Table S2).[27,28,39,60]

Water contamination is another potential source for LiOH,[19,20] and efforts were made in order to minimize this in our study (see Experimental Methods in the Supporting

Information). Interestingly, adding 1% H_2O to the electrolyte while plating/stripping lithium in an Ar environment showed no improvement to the CE nor suppressed dendritic growth (Figure S17), suggesting that LiOH formed from H_2O is not responsible for the large improvements to Coulombic efficiency seen when cycling in an O_2 environment. This result has significant implications for understanding lithium−air batteries in the presence of water: multiple studies have shown that these cells cycle even when the Li metal electrode is not protected.[11,38,61] The results presented here indicate that O_2 and not simply water is key in protecting the Li metal (Figure S18).

In conclusion, our work demonstrated improved Coulombic efficiencies when cycling lithium in the presence of O_2. Even in a mixed O_2/N_2 gas environment—with an O_2/N_2 ratio close to that in air (and in a dry room)—O_2 helped form a more homogeneous LiOH-containing SEI layer on the Cu substrate surface, enabling uniform Li nucleation and improving subsequent plating−stripping efficiencies. While LiOH is the major component of the SEI, it is the SEI formed in the presence of O_2 rather than water that is key to the improved performance. In the absence of O_2 or other additives, a more heterogeneous SEI is formed containing a more diverse range of species, which results in nonuniform plating and dendrite growth. Gas crossover could therefore potentially be used as a pretreatment method for promoting homogeneous SEI layers in Li metal anodes. The effects of gas crossover on SEI formation and overall cell performance posit design questions for electrode fabrication in future Li metal batteries, including practical Li−air batteries.

ASSOCIATED CONTENT

Supporting Information

The Supporting Information is available free of charge at https://pubs.acs.org/doi/10.1021/acsenergylett.0c00257.

Experimental methods and supplemental figures and tables (PDF)

AUTHOR INFORMATION

Corresponding Author

Clare P. Grey − *Department of Chemistry, University of Cambridge, Cambridge CB2 1EW, U.K.;* orcid.org/0000-0001-5572-192X; Phone: (+44)1223336509; Email: cpg27@cam.ac.uk; Fax: (+44)1223336362

Authors

Evelyna Wang − *Department of Chemistry, University of Cambridge, Cambridge CB2 1EW, U.K.;* orcid.org/0000-0002-5697-474X

Sunita Dey − *Department of Chemistry, University of Cambridge, Cambridge CB2 1EW, U.K.*

Tao Liu − *Department of Chemistry, University of Cambridge, Cambridge CB2 1EW, U.K.;* orcid.org/0000-0002-6515-0427

Svetlana Menkin − *Department of Chemistry, University of Cambridge, Cambridge CB2 1EW, U.K.*

Complete contact information is available at: https://pubs.acs.org/10.1021/acsenergylett.0c00257

Notes

The authors declare no competing financial interest.

ACKNOWLEDGMENTS

The authors thank EPSRC-EP/M009521/1 and the Cambridge Trust (E.W.) for research funding. The X-ray photoelectron (XPS) data collection was performed at the EPSRC National Facility for XPS ("HarwellXPS"), operated by Cardiff University and UCL, under Contract No. PR16195.

REFERENCES

(1) Yu, S. H.; Feng, X.; Zhang, N.; Seok, J.; Abruña, H. D. Understanding Conversion-Type Electrodes for Lithium Rechargeable Batteries. *Acc. Chem. Res.* **2018**, *51* (2), 273−281.

(2) Aurbach, D.; McCloskey, B. D.; Nazar, L. F.; Bruce, P. G. Advances in Understanding Mechanisms Underpinning Lithium-Air Batteries. *Nat. Energy* **2016**, *1*, 16128.

(3) Li, Y.; Lu, J. Metal-Air Batteries: Will They Be the Future Electrochemical Energy Storage Device of Choice? *ACS Energy Lett.* **2017**, *2* (6), 1370−1377.

(4) Lee, J.-S.; Kim, S. T.; Cao, R.; Choi, N.-S.; Liu, M.; Lee, K. T.; Cho, J. Metal-Air Batteries with High Energy Density: Li-Air versus Zn-Air. *Adv. Energy Mater.* **2011**, *1* (1), 34−50.

(5) Geng, D.; Ding, N.; Hor, T. S. A.; Chien, S. W.; Liu, Z.; et al. From Lithium-Oxygen to Lithium-Air Batteries : Challenges and Opportunities. *Adv. Energy Mater.* **2016**, *6*, 1502164.

(6) Yao, X.; Dong, Q.; Cheng, Q.; Wang, D. Why Do Lithium−Oxygen Batteries Fail: Parasitic Chemical Reactions and Their Synergistic Effect. *Angew. Chem., Int. Ed.* **2016**, *55* (38), 11344−11353.

(7) Abraham, K. M.; Jiang, Z. A. Polymer Electrolyte-Based Rechargeable Lithium/Oxygen Battery. *J. Electrochem. Soc.* **1996**, *143* (1), 1−5.

(8) Gao, X.; Chen, Y.; Johnson, L. R.; Jovanov, Z. P.; Bruce, P. G. A Rechargeable Lithium-Oxygen Battery with Dual Mediators Stabilizing the Carbon Cathode. *Nat. Energy* **2017**, *2*, 17118.

(9) Zhou, B.; Guo, L.; Zhang, Y.; Wang, J.; Ma, L.; Zhang, W.-H.; Fu, Z.; Peng, Z. A High-Performance Li-O2 Battery with a Strongly Solvating Hexamethylphosphoramide Electrolyte and a LiPON-Protected Lithium Anode. *Adv. Mater.* **2017**, *29*, 1701568.

(10) Liu, T.; Liu, Z.; Kim, G.; Frith, J. T.; Garcia-Araez, N.; Grey, C. P. Understanding LiOH Chemistry in a Ruthenium-Catalyzed Li-O2 Battery. *Angew. Chem., Int. Ed.* **2017**, *56*, 16057−16062.

(11) Liu, T.; Leskes, M.; Yu, W.; Moore, A. J.; Zhou, L.; Bayley, P. M.; Kim, G.; Grey, C. P. Cycling Li-O2 Batteries via LiOH Formation and Decomposition. *Science (Washington, DC, U. S.)* **2015**, *350* (6260), 530−533.

(12) Xiao, J.; Wang, D.; Xu, W.; Wang, D.; Williford, R. E.; Liu, J.; Zhang, J.-G. Optimization of Air Electrode for Li/Air Batteries. *J. Electrochem. Soc.* **2010**, *157* (4), A487−A492.

(13) Mahne, N.; Schafzahl, B.; Leypold, C.; Leypold, M.; Grumm, S.; Leitgeb, A.; Strohmeier, G. A.; Wilkening, M.; Fontaine, O.; Kramer, D.; et al. Singlet Oxygen Generation as a Major Cause for Parasitic Reactions during Cycling of Aprotic Lithium-Oxygen Batteries. *Nat. Energy* **2017**, *2* (5), 17036.

(14) Park, J. B.; Lee, S. H.; Jung, H. G.; Aurbach, D.; Sun, Y. K. Redox Mediators for Li−O2 Batteries: Status and Perspectives. *Adv. Mater.* **2018**, *30* (1), 1704162.

(15) Hojberg, J.; McCloskey, B. D.; Hjelm, J.; Vegge, T.; Johansen, K.; Norby, P.; Luntz, A. C. An Electrochemical Impedance Spectroscopy Investigation of the Overpotentials in Li-O2 Batteries. *ACS Appl. Mater. Interfaces* **2015**, *7*, 4039−4047.

(16) Peled, E.; Menkin, S. Review - SEI: Past, Present and Future. *J. Electrochem. Soc.* **2017**, *164* (7), A1703−A1719.

(17) Pei, A.; Zheng, G.; Shi, F.; Li, Y.; Cui, Y. Nanoscale Nucleation and Growth of Electrodeposited Lithium Metal. *Nano Lett.* **2017**, *17*, 1132−1139.

(18) Ding, N.; Zhou, L.; Zhou, C.; Geng, D.; Yang, J.; Chien, S. W.; Liu, Z.; Ng, M. F.; Yu, A.; Hor, T. S. A.; et al. Building Better Lithium-Sulfur Batteries: From LiNO2 to Solid Oxide Catalyst. *Sci. Rep.* **2016**, *6* (1), 33154.

(19) Shui, J. L.; Okasinski, J. S.; Kenesei, P.; Dobbs, H. A.; Zhao, D.; Almer, J. D.; Liu, D. J. Reversibility of Anodic Lithium in Rechargeable Lithium-Oxygen Batteries. *Nat. Commun.* **2013**, *4*, 2255.

(20) Sun, F.; Gao, R.; Zhou, D.; Osenberg, M.; Dong, K.; Kardjilov, N.; Hilger, A.; Markötter, H.; Bieker, P. M.; Liu, X.; et al. Revealing Hidden Facts of Li Anode in Cycled Lithium−Oxygen Batteries through X-Ray and Neutron Tomography. *ACS Energy Lett.* **2019**, *4* (1), 306−316.

(21) Assary, R. S.; Lu, J.; Du, P.; Luo, X.; Zhang, X.; Ren, Y.; Curtiss, L. A.; Amine, K. The Effect of Oxygen Crossover on the Anode of a Li-O2 Battery Using an Ether-Based Solvent: Insights from Experimental and Computational Studies. *ChemSusChem* **2013**, *6*, 51−55.

(22) Younesi, R.; Hahlin, M.; Roberts, M.; Edstrom, K. The SEI Layer Formed on Lithium Metal in the Presence of Oxygen: A Seldom Considered Component in the Development of the Li-O2 Battery. *J. Power Sources* **2013**, *225*, 40−45.

(23) Inaba, M.; Kinumoto, T.; Kiriake, M.; Umebayashi, R.; Tasaka, A.; Ogumi, Z. Gas Crossover and Membrane Degradation in Polymer Electrolyte Fuel Cells. *Electrochim. Acta* **2006**, *51* (26), 5746−5753.

(24) Gittleson, F. S.; Jones, R. E.; Ward, D. K.; Foster, M. E. Oxygen Solubility and Transport in Li-Air Battery Electrolytes: Establishing Criteria and Strategies for Electrolyte Design. *Energy Environ. Sci.* **2017**, *10*, 1167−1179.

(25) Hartmann, P.; Grubl, D.; Sommer, H.; Janek, J.; Bessler, W. G.; Adelhelm, P. Pressure Dynamics in Metal-Oxygen (Metal-Air) Batteries: A Case Study on Sodium Superoxide Cells. *J. Phys. Chem. C* **2014**, *118*, 1461−1471.

(26) Lindberg, J.; Endrodi, B.; Avall, G.; Johansson, P.; Cornell, A.; Lindbergh, G. Li Salt Anion Effect on O2 Solubility in an Li-O2 Battery. *J. Phys. Chem. C* **2018**, *122*, 1913−1920.

(27) Schiemann, M.; Bergthorson, J.; Fischer, P.; Scherer, V.; Taroata, D.; Schmid, G. A Review on Lithium Combustion. *Appl. Energy* **2016**, *162*, 948−965.

(28) Barnett, D. S.; Gil, T. K.; Kazimi, M. S. Lithium Mixed-Gas Reactions. *Fusion Technol.* **1989**, *15* (2P2B), 967−972.

(29) Wang, H.; Zhang, W. D.; Deng, Z. Q.; Chen, M. C. Interaction of Nitrogen with Lithium in Lithium Ion Batteries. *Solid State Ionics* **2009**, *180*, 212−215.

(30) McFarlane, E. F.; Tompkins, F. C. Nitridation of Lithium. *Trans. Faraday Soc.* **1962**, *58*, 997−1007.

(31) Momma, T.; Nara, H.; Yamagami, S.; Tatsumi, C.; Osaka, T. Effect of the Atmosphere on Chemical Composition and Electrochemical Properties of Solid Electrolyte Interface on Electrodeposited Li Metal. *J. Power Sources* **2011**, *196*, 6483−6487.

(32) Stark, J.; Ding, Y.; Kohl, P. A. Role of Dissolved Gas in Ionic Liquid Electrolytes for Secondary Lithium Metal Batteries. *J. Phys. Chem. C* **2013**, *117*, 4980−4985.

(33) Li, Y.; Li, Y.; Sun, Y.; Butz, B.; Yan, K.; Koh, A. L.; Zhao, J.; Pei, A.; Cui, Y. Revealing Nanoscale Passivation and Corrosion Mechanisms of Reactive Battery Materials in Gas Environments. *Nano Lett.* **2017**, *17*, 5171−5178.

(34) Bieker, G.; Winter, M.; Bieker, P. Electrochemical in Situ Investigations of SEI and Dendrite Formation on the Lithium Metal Anode. *Phys. Chem. Chem. Phys.* **2015**, *17*, 8670−8679.

(35) Wood, K. N.; Kazyak, E.; Chadwick, A. F.; Chen, K.-H.; Zhang, J.-G.; Thornton, K.; Dasgupta, N. P. Dendrites and Pits: Untangling the Complex Behavior of Lithium Metal Anodes through Operando Video Microscopy. *ACS Cent. Sci.* **2016**, *2*, 790−801.

(36) Aurbach, D.; Weissman, I.; Zaban, A.; Chusid, O. Correlation Between Surface Chemistry, Morphology, Cycling Efficiency and Interfacial Properties of Li Electrodes in Solutions Containing Different Li Salts. *Electrochim. Acta* **1994**, *39*, 51−71.

(37) Qiu, F.; Zhang, X.; Qiao, Y.; Zhang, X.; Deng, H.; Shi, T.; He, P.; Zhou, H. An Ultra-Stable and Enhanced Revesibility Lithium Metal Anode with a Sufficient O2 Design for Li-O2 Battery. *Energy Storage Mater.* **2018**, *12*, 176−182.

(38) Aurbach, D. The Correlation Between Surface Chemistry, Surface Morphology, and Cycling Efficiency of Lithium Electrodes in a Few Polar Aprotic Systems. *J. Electrochem. Soc.* **1989**, *136* (11), 3198.

(39) Giordani, V.; Walker, W.; Bryantsev, V. S.; Uddin, J.; Chase, G. V.; Addison, D. Synergistic Effect of Oxygen and LiNO3 on the Interfacial Stability of Lithium Metal in a Li/O2 Battery. *J. Electrochem. Soc.* **2013**, *160* (9), A1544−A1550.

(40) Kim, Y.; Koo, D.; Ha, S.; Jung, S. C.; Yim, T.; Kim, H.; Oh, S. K.; Kim, D.-M.; Choi, A.; Kang, Y.; et al. Two-Dimensional Phosphorene-Derived Protective Layers on a Lithium Metal Anode for Lithium-Oxygen Batteries. *ACS Nano* **2018**, *12* (5), 4419−4430.

(41) Lu, D.; Tao, J.; Engelhard, M. H.; Zheng, J.; Yan, P.; Wang, C.; Liu, B.; Xu, W.; Zhang, J.-G. Enhanced Cyclability of Lithium-Oxygen Batteries with Electrodes Protected by Surface Films Induced via In Situ Electrochemical Process. *Adv. Energy Mater.* **2018**, *8* (11), 1702340.

(42) Farooqui, U. R.; Ahmad, A. L.; Hamid, N. A. Challenges and Potential Advantages of Membranes in Lithium Air Batteries: A Review. *Renewable Sustainable Energy Rev.* **2017**, *77*, 1114−1129.

(43) Roberts, M.; Younesi, R.; Richardson, W.; Liu, J.; Zhu, J.; Edstr, K. Increased Cycling Efficiency of Lithium Anodes in Dimethyl Sulfoxide Electrolytes For Use in Li-O_2 Batteries. *ECS Electrochem. Lett.* **2014**, *3* (6), 62−65.

(44) Asadi, M.; Sayahpour, B.; Abbasi, P.; Ngo, A. T.; Karis, K.; Jokisaari, J. R.; Liu, C.; Narayanan, B.; Gerard, M.; Yasaei, P.; et al. A Lithium-Oxygen Battery with a Long Cycle Life in an Air-like Atmosphere. *Nature* **2018**, *555* (7697), 502−506.

(45) Aurbach, D.; Granot, E. The Study of Electrolyte Solutions Based on Solvents from the "Glyme" Family (Linear Polyethers) for Secondary Li Battery Systems. *Electrochim. Acta* **1997**, *42* (4), 697−718.

(46) Camacho-Forero, L. E.; Balbuena, P. B. Elucidating Electrolyte Decomposition under Electron-Rich Environments at the Lithium-Metal Anode. *Phys. Chem. Chem. Phys.* **2017**, *19* (45), 30861−30873.

(47) Saito, M.; Fujinami, T.; Yamada, S.; Ishikawa, T.; Otsuka, H.; Ito, K.; Kubo, Y. Effects of Li Salt Anions and O2 Gas on Li Dissolution/Deposition Behavior at Li Metal Negative Electrode for Non-Aqueous Li-Air Batteries. *J. Electrochem. Soc.* **2017**, *164* (12), A2872−A2880.

(48) Xu, C.; Sun, B.; Gustafsson, T.; Edstrom, K.; Brandell, D.; Hahlin, M. Interface Layer Formation in Solid Polymer Electrolyte Lithium Batteries: An XPS Study. *J. Mater. Chem. A* **2014**, *2*, 7256−7264.

(49) Schmitz, R.; Ansgar Müller, R.; Wilhelm Schmitz, R.; Schreiner, C.; Kunze, M.; Lex-Balducci, A.; Passerini, S.; Winter, M. SEI Investigations on Copper Electrodes after Lithium Plating with Raman Spectroscopy and Mass Spectrometry. *J. Power Sources* **2013**, *233*, 110−114.

(50) Jurng, S.; Brown, Z. L.; Kim, J.; Lucht, B. L. Effect of Electrolyte on the Nanostructure of the Solid Electrolyte Interphase (SEI) and Performance of Lithium Metal Anodes. *Energy Environ. Sci.* **2018**, *11* (9), 2600−2608.

(51) Zhang, X.-Q.; Cheng, X.-B.; Chen, X.; Yan, C.; Zhang, Q. Fluoroethylene Carbonate Additives to Render Uniform Li Deposits in Lithium Metal Batteries. *Adv. Funct. Mater.* **2017**, *27*, 1605989.

(52) Andersson, A. M.; Edström, K. Chemical Composition and Morphology of the Elevated Temperature SEI on Graphite. *J. Electrochem. Soc.* **2001**, *148* (10), 1100−1109.

(53) Ko, J.; Yoon, Y. S. Recent Progress in LiF Materials for Safe Lithium Metal Anode of Rechargeable Batteries: Is LiF the Key to Commercializing Li Metal Batteries? *Ceram. Int.* **2019**, *45* (1), 30−49.

(54) Zhang, X. Q.; Chen, X.; Xu, R.; Cheng, X. B.; Peng, H. J.; Zhang, R.; Huang, J. Q.; Zhang, Q. Columnar Lithium Metal Anodes. *Angew. Chem., Int. Ed.* **2017**, *56* (45), 14207−14211.

(55) Peled, E.; Golodnitsky, D.; Ardel, G. Advanced Model for Solid Electrolyte Interphase Electrodes in Liquid and Polymer Electrolytes. *J. Electrochem. Soc.* **1997**, *144* (8), L208.

(56) Sharon, D.; Hirshberg, D.; Afri, M.; Garsuch, A.; Frimer, A. A.; Aurbach, D. Lithium-Oxygen Electrochemistry in Non-Aqueous Solutions. *Isr. J. Chem.* **2015**, *55*, 508−520.

(57) Bryantsev, V. S.; Uddin, J.; Giordani, V.; Walker, W.; Addison, D.; Chase, G. V. The Identification of Stable Solvents for Nonaqueous Rechargeable Li-Air Batteries. *J. Electrochem. Soc.* **2013**, *160* (1), A160−A171.

(58) Schwenke, K. U.; Meini, S.; Wu, X.; Gasteiger, H. A.; Piana, M. Stability of Superoxide Radicals in Glyme Solvents for Non-Aqueous Li-O2 Battery Electrolytes. *Phys. Chem. Chem. Phys.* **2013**, *15*, 11830−11839.

(59) Freunberger, S. A.; Chen, Y.; Drewett, N. E.; Hardwick, L. J.; Barde, F.; Bruce, P. G. The Lithium-Oxygen Battery with Ether-Based Electrolytes. *Angew. Chem., Int. Ed.* **2011**, *50* (37), 8609−9613.

(60) Shang, J.; Shirazian, S. Facilitated Dissociation of Water in the Presence of Lithium Metal at Ambient Temperature as a Requisite for Lithium-Gas Reactions. *J. Phys. Chem. C* **2018**, *122*, 16016−16022.

(61) Togasaki, N.; Momma, T.; Osaka, T. Enhancement Effect of Trace H2O on the Charge-Discharge Cycling Performance of a Li Metal Anode. *J. Power Sources* **2014**, *261*, 23−27.